Journal of research in engineering and its applications

Vol. 1, Issue. 1, (2018), pp. 16-26

A Novel Method for SBI Segmentation and Cramer-Rao Bound Condition for Histogram Equalization In Medical Image Processing

Partheban .C [1], *Sandhya Madhavan* [2]

Research Scholar,REVA University,Bangalore, Karnataka, India [1]

Email: parthi09@gmail.com

Associate Professor, Motilal Nehru National Institute of Technology, Allahabad, Uttar Pradesh, India [2],

Email: sandhya.m@gmail.com

Abstract

Image processing is widely accepted in the field of medical image processing for improvement in image for detection of disease in earlier stage. Image processing with respect to time factor provides appropriate detection of tumors in different cancer detection. In cancer detection process important factors considered are accuracy and quality of the image with minimal processing time. This requirement leads to the challenge of image processing technique with effective mechanism. In this research proposed a appropriate mechanism for improving processing time and accuracy for breast cancer. To improve the accurate detection of tumor extraction is adopted Cramer-Rao mechanism based on the intensity of the pixel. For the further efficiency improvisation of breast cancer detection straighten boundary (SBI) approach is adopted for cancer edge detection. In final stage for the extracted part through SBI and Cramer-rao approach histogram equalization is adopted. Simulation results reveals that

Keywords: *Cramer – Rao, Straighten Boundary Condition, Histogram Equalization,*

1.INTRODUCTION

Cancer is simply an abnormal growth of cells. The body cells divide in a continuous manner and invade to surrounding tissues. It is named after the part from which it is originated (Vidya, V. K., & Mathew, S., 2016). Cancer is generally classified as benign and malignant masses. The benign ones are simple cysts which do not advance to the nearby tissues. It implies that they are not cancerous in nature. Whereas malignant masses spread to other parts of the body and grow in other organs and bones. Breast cancer which starts as a breast lump is the leading cancer diagnosed among women. In the western countries the surveys shows that one out of 11 women is suffering from breast cancer at some stages in their life. Most of the times breast cancer do not show any symptoms in the initial stages. In later stages it can be change in the breast shape, dimpling of the skin, fluid coming from the nipple, or a red scaly patch of skin. The early detection and timely medical treatment are the only factors responsible for the long term survival of breast cancer patients. X ray mammography is considered as the golden standard tool for breast cancer detection. But it is possessed with high false negative and positive rate. It is not applicable in the case of women with dense breast tissue

(Huynh, P. T et al., 1998). Statistical model of texture consider mammographic appearance as a spatially variable structure. It is not widely used since the synthesis speed is very low in this method (Rose, C. J., & Taylor, C. J., 2003).

MRI is an efficient method for certain high risk cases. But the lesion sensitivity and specificity determines the overall accuracy of this method (Brockway, J et al., 2004). Microwave imaging is accompanied by a significant amount of backscatter which falsifies the image (Abbosh, Y. M., 2014). Electrical impedance tomography is associated with high cost (Campisi, M. S et al., 2014). Ultra Sound are generally said to be complex because of data decomposition, it can be described in terms of speckle information. Ultra sound imaging method utilizes high frequency sound waves to explore inner parts of the body. It is a non destructive and noninvasive technology. Which means it does not alter the target being tested and do not cause any pain or discomfort. Ultra sound waves are emitted from a transmitter to the object which will reflect back if there is an impurity or a crack. The resultant echoes are analyzed to extract different parameters. High detection resolution, low cost and high flexibility are the other advantages of ultra sound imaging. Ultrasound imaging (UT) has proved effective for softtissue characterization. It uses Computer Aided Design for classification. Lesion segmentation plays a crucial role in the CAD system since the computation of features related to lesion shape is largely dependent on the accuracy of segmentations (Tan, T et al., 2012). Radial Gradient Index (RGI) filtering technique is used to detect lesions on breast ultrasound images automatically. In this method images are sub-sampled by a factor of 4. The overlap between lesions reduces the accuracy of this method. Watershed segmentation can be used for initial lesion detection. But the Region of Interest obtained through this method is not correct which falsifies the further processes (Hoon, M., & Yap, M ., 2008). Edge detection is employed to define Region of Interest in a particular method. But the efficiency of this method is much depended on the type of edge detection algorithm used (. Automated breast Ultrasound using adaptive threshold is used for multi-dimensional tumor detection. The overall efficiency of this method relies upon the threshold selected (Vidya, V. K., & Mathew, S ., 2016).Feed forward back propagation neural network is another method used to classify benign and malignant breast tumor. Here Levenberg-Marquardt (LM) is used as the training algorithm. The accuracy of this technique is defined as the ratio of the number of samples correctly classified to the total number of samples tested (Su, Y et al., 2011).

2.RELATED WORKS

The existing research work carried out in the cancer image processing application are reviewed (Kusakunniran, W et al., 2016) proposed a requires two main steps which will be focused in this paper. They are the quality assessment and the segmentation of diabetic retinopathy images. In the image quality assessment, four features (namely color, contrast, focus, and illumination) have been investigated. As a result, the contrast histogram in the Principal Component Analysis (PCA) space is used. In the image segmentation, the histogram equalization is used in the pre-processing. Then, the image segmentation based on the iterative selection and the grabcut algorithm is applied. The experimental results demonstrate that the proposed method can achieve very promising performance. Wen, H et al., 2016 developed an image enhancement algorithm which based on wavelet domain homomorphic filtering and contrast limited adaptive histogram equalization (CLAHE). Firstly, the image is decomposed by wavelet

transformation, the image is decomposed into low-frequency and high-frequency coefficients of 1st layer of wavelet domain. Then the low frequency coefficients are processed by an improved homomorphic filter, and then linear amplified. The high frequency coefficients are processed by wavelet threshold shrinkage, and then the wavelet reconstruction is performed. Finally, the contrast limited adaptive histogram equalization (CLAHE) is used to modify the image's histogram, and the processing of the image is completed. The quality of image enhancement is carried on the subjective and objective evaluation, and compared with some other enhancement algorithms. Experimental results show that the algorithm can effectively enhance the texture detail of medical X-ray images, increasing the brightness and contrast, suppress noise, better than the general traditional enhancement algorithms. Kaur, H., & Rani, J., 2016 examined and look at different Histogram based enhancement techniques. Histogram equalization analyze on the bases of Magnetic resonance imaging (MRI) furthermore calculate the metrics parameter of histogram techniques. Image enhancement is a procedure of changing or adjusting image in order to make it more suitable for certain applications and is used to enhance or improve contrast ratio, brightness of image, remove noise from image and make it easier to identify. Magnetic resonance imaging (MRI) is an astounding medical technology provide more appropriate information regarding Human brain soft tissue, cancer, stroke and various another diseases. MRI helps doctors to identify the diseases easily. MRI has very low contrast ratio to improve contrast of MRI image we used Histogram equalization technique. In which, Histogram Equalization, Local Histogram Equalization, Adaptive Histogram Equalization and Contrast Limited Adaptive Histogram Equalization techniques are compared. Shajy, L et al., 2014 evaluated the conventional HE enhancement process outputted an excessive contrast result. Which leads to poor classification result, especially in medical image processing. In this paper we discussed about various HE methods for the enhancement of sputum cytology images. Our ultimate aim is, to develop an efficient algorithm to detect lung cancer at early stage. The challenging problem, we faced, in this work is to find out a proper algorithm for the enhancement of sputum cytology images. Here we consider some famous HE algorithm for the enhancement of sputum cytology images. The Recursive Mean Separate Histogram Equalization Method (RMSHE) gives result in sputum cytology image enhancement. Huang, L et al., 2013 performed Histogram equalization is a significant application for image gray level transformation, which is widely used in image enhancement processing. We adopt keeping encrypted histogram-equalized image data in the database as the security strategy for our personal healthcare information cloud platform system. Three kinds of symmetric encryption algorithms are used to test histogram equalized image. The experiment results show AES encryption algorithm suitable for our personal healthcare information system. Senthilkumaran, N., & Thimmiaraja, J., 2014 investigated magnetic resonance imaging (MRI) is an advanced medical imaging technique providing rich information about the human soft tissue anatomy. MRI of the brain is an invaluable tool to help physicians to diagnose and treat various brain diseases including stroke, cancer, and epilepsy. The specific information to evaluate the diseases. Histogram equalization is one of the important steps in image enhancement technique for MRI. There are several methods of image enhancement and each of them is needed for a different type of analysis. In this paper study and compare different Techniques like Global Histogram Equalization (GHE), Local histogram equalization (LHE), Brightness preserving Dynamic Histogram equalization

(BPDHE) and Adaptive Histogram Equalization (AHE) using different objective quality measures for MRI brain image Enhancement.

3.METHODOLOGY

The aim of this research to effectively perform the medical image processing for cancer application. As per the review of existing report it is identified that cancer disease is severe threat to human begins life. Hence in this research concentrate on examining and analyzing cancer disease image processing especially breast cancer. In breast cancer detection images are occurred from mammogram and undergo processing. The data for the breast image processing are collected and processed using proposed approach. In figure 1 overview flowchart of the proposed approach is presented. In the primary stage of the image processing image data are collected by use of mammogram image acquisition method which is followed by conventional image enhancement approach.

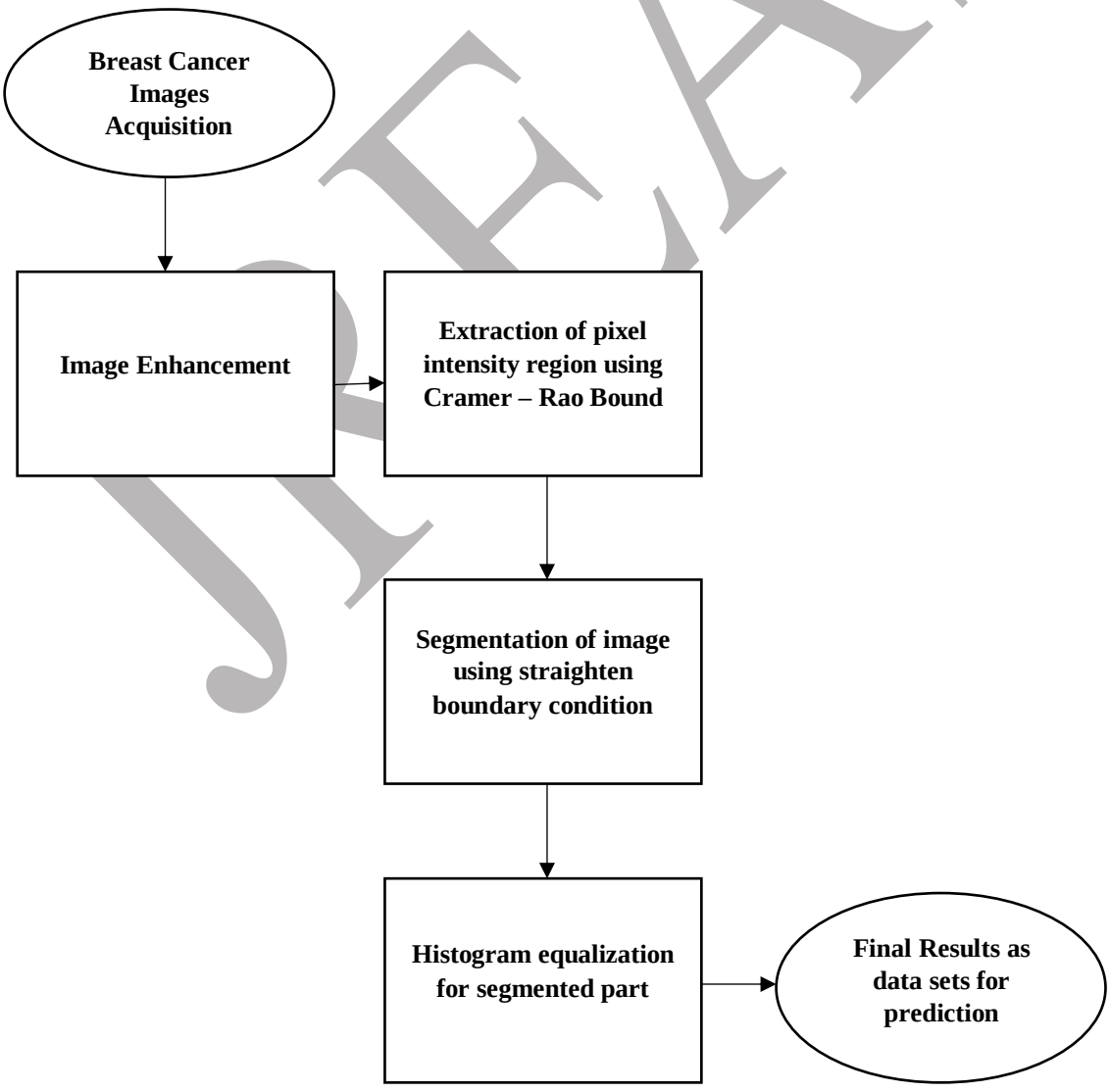

In the next stage of the image processing to improve the performance of the cancer detection based on the intensity. The intensity values in the images is used for cancer detection based on the Cramer – Rao method based on upper bound and lower bound condition. Based on this intensity pixels within the lower bound range of pixel with higher pixel intensity to lower intensity. After the identification of pixel intensity with the specified range the cancer affected part need to be segmented for increasing the processing time and cancer detection efficiency. Since the main objective of this research is to improve the brest cancer detection accuracy for the segmented part based on straighten boundary condition cancer affected image is histogram equalized and final dataset were created. In Cramer-Rao approach through the mathematical formulation intensity of the pixel will identified and provided the value of the cancer affected pixel intensity for extraction of cancer affected region. Through the extraction of intensity pixel by cramer-rao rule image part are segmented using SBI condition. From the segmented part images affected with cancer in mammogram images can be identified effectively with minimal time. The image intensity pixel with cancer are stored in a separate datasets for future processing.

3.1 Calculation of CRB (Cramer- Rao Bound)

A classical problem in statistical signal processing consists of recovering a signal x from a vector of Q observations

$$y = x + w$$

where w is a noise vector. Here, we assume that $w \in \mathbb{C}^Q$ is a realization of a circular Gaussian random noise vector W with zero-mean and covariance matrix $\Gamma = \mathrm{E}[WW^H] \in \mathbb{C}^{Q\times Q}$ ($(\cdot)^H$ denotes the transconjugate operation). We assume that the signal $x \in \mathbb{C}^Q$ admits a sparse representation in a finite dictionary $\mathcal{E} = \{e_\upsilon \mid \upsilon \in \mathbb{R}\}$ of vectors of $\mathbb{C}^Q$ which are parameterized by a scalar variable $\upsilon \in \mathbb{R}$. More precisely, there exist $M \in \mathbb{N}*$, $c = [c1,...,] \top \in (\mathbb{C}*)M$ and $\nu = [\nu 1,...,\nu M] \top \in \mathbb{R}M$ such that

$$x = \sum_{n=1}^{M} c_n e_{\nu n} = [e_{\nu 1} \dots] = Ec$$

The vector $y \in \mathbb{C}^Q$ is thus a realization of a random vector Y with probability density function

$$\mathrm{p}Y\,|_{c,\nu}(y) = (1/(\pi)^M(\det(\Gamma))^{1/2})*\exp(-(y-Ec)^H\Gamma^{-1}(y-Ec))$$

In the following, it is assumed that $\upsilon \rightarrow e\upsilon$ is a twice differentiable function.

3.2 Calculation of the CRB

Up to an additive constant, the negative-log-likelihood is equal to

$$\mathcal{L}(y \mid c, \nu) = w^H\Gamma^{-1}w$$

In the following w_R and w_I denote the real part and the imaginary part of w, a similar notation being used for other complex-valued vectors and matrices.

Let us first look at the expression of the Wirtinger's derivative [7] of the neg-log-likelihood with respect to the conjugate of c:

$$\partial\mathcal{L}(y \mid c, v) / \partial c^* = 1/2 \left((\partial\mathcal{L}(y \mid c, v) / \partial c_R + \iota\, \partial\mathcal{L}(y \mid c, v) \partial c_I) \right) = -EH\Gamma^{-1}w$$

We have then

$$(\partial^2\mathcal{L}(y \mid c, v) / \partial c_R \partial c^\top{}_R) = -2\, \partial \left({}^\top{}_R (\Gamma^{-1}E)_R + w^\top{}_I (\Gamma^{-1}E)_I \right) \partial_{cR}$$

$$= 2\, \mathrm{Re}\{E^H\Gamma^{-1}E\}$$

and, by similar calculations,

$$(\partial^2\mathcal{L}(y \mid c, v) / \partial c_R \partial c^\top{}_I) = -2\, \mathrm{Im}\{E^H\Gamma^{-1}E\}$$

$$(\partial^2\mathcal{L}(y \mid c, v) / \partial c_I \partial c^\top{}_I) = 2\, \mathrm{Re}\{E^H\Gamma^{-1}E\}$$

On the other hand, the neg-log-likelihood can be re-expressed as

$$\mathcal{L}(y \mid c, v) = \left(y - \sum_{n=1}^{M} c_n e_{vn} \right) H\, \Gamma^{-1} \left(y - \sum_{n=1}^{M} c_n e_{vn} \right)$$

For every $n \in \{1,...,\}$, this leads to

$$(\partial\mathcal{L}(y \mid c, v)\, \partial_{vn}) = -2\, \mathrm{Re}\{c^*{}_n (e'{}_{vn})^H \Gamma^{-1} w\}$$

where $e'\, vn$ is the gradient of $v \rightarrow e_v$ at v_n.

For the second-order derivatives, we deduce that, for every $(n, m) \in \{1,...,\}^2$,

$$(\partial^2\mathcal{L}(y \mid c, v) / \partial v_n \partial v_m = 2(\mathrm{Re}\{c*{}_n c_m (e'{}_{vn})^H \Gamma^{-1} e'{}_{vm}\} - \mathrm{Re}\{c*{}_n (e''{}_{vn})^H \Gamma^{-1} w\} \delta_{n-m})$$

$$(\partial^2\mathcal{L}(y \mid c, v) / \partial v_n \partial c*{}_m = 1/2\, (\partial^2\mathcal{L}(y \mid c, v) / \partial v_n \partial c_{R,m} + \iota\, \partial^2\mathcal{L}(y \mid c, v) \partial v_n \partial c_{I,m})$$

$$= c_n e^H{}_{vm} \Gamma^{-1} e'{}_{vn} - (e' \quad)^H \Gamma^{-1} w\, \delta_{n-m}$$

$\mathcal{F}_p = \mathrm{E}\, [\partial^2\mathcal{L}(Y \mid c, v) / \partial_p \partial_p{}^\top\,] \in \mathbb{R}^{3M \times 3M}$.

Since W is zero-mean, which yield, for every $(n, m) \in \{1,...,\}^2$,

3.3 Histogram Equalization

Histogram equalization is a process of flattening the histogram, where the distribution of the value of the degrees of gray in an image made flat. To be able to perform a histogram equalization is necessary which the

cumulative distribution function of the cumulative histogram is. Histogram equalization is used to improve the quality of segmentation. Excessive segmentation is a major problem facing the segmentation using watershed algorithm because it needed a good preprocessing to avoid excessive segmentation. Value histogram equalization results are as follows (Radhiyah, A et al., 2016):

$$w = \frac{c_w . t_h}{f_{lx} . f_{ly}}$$

Where, w - value of gray histogram results

c_w - Cumulative histogram of w

t_h - Threshold degrees of gray

$f_{lx} . f_{ly}$ - Image size

3.4 Histogram Equalization in Image Processing

In the past, multiple contrast enhancement techniques were developed for image visualization. We can categorize them into two groups mainly, the spatial domain- based technique and the transformation- based technique. Spatial domain are implemented directly with the image pixels (Mundhada, S. O., & Shandilya, V. K., 2012). Some of the examples are the basic histogram equalization (HE) and the modified HE which can be further categorized into the global histogram equalization (GHE) and local HE- based methods (Koh, N. C. Y et al., 2016; Lidong, H et al., 2015).

In the basic HE technique, HE initially computes the probability distribution function (PDF) from the image histogram. The cumulative distribution function (CDF) is calculated and then plug in to the transfer function of an image. Next, the new distribution of gray level is remapped based on the respective CDF. The probability of occurrence of a pixel of level k in the image is:

$$P_x(k) = \frac{n_k}{n}$$

Where n_k is the number of pixels at level k and n is the sum number of pixels in the image. The formula of CDF of the image is:

$$cdfx(k) = \sum_{j=0}^{t} P_x(k)$$

Applying the transformation function:

$$TF = (cdfx(k))(x_{\max} - x_{\min}) + x_{\min}$$

Where $x_{\max}$ is the maximum gray level and $x_{\min}$ is the minimum gray level of the output image. The HE stretches the high probability levels better than low probability levels and therefore allowing areas of lower local contrast such as the brain lesion to gain a better contrast. However, HE constantly distributes the output histogram using a cumulated histogram to produce an overly enhanced image.

To overcome the problem, the GHE modified technique such as the extreme level eliminating histogram equalization (ELEHE) proposed by Tan et al., and adaptive gamma correction with weighting distribution (AGCWD) proposed by Shih et al., was introduced. The ELEHE technique eliminates the two extreme grayscale levels, 0 and 255 while normalizing the resultant distribution and finally maps the transfer function on the image (Tan, T. L et al., 2012). In AGCWD technique, the authors brightens the image using the gamma correction and the probability distribution of luminance pixels (Huang, S. C et al., 2013). The ELEHE produces a darken lesion area but also darkens the other tissue areas making it difficult to detect the brain lesion while the AGCWD brightens the image but brain image details are loss. On the contrary, the LHE technique such as the contrast limited adaptive histogram equalization (CLAHE) (Pizer, S. M et al., 1987) proposed by Pizer et al., and extreme level adaptive eliminating histogram equalization (ELEAHE) (Tan, T. L et al., 2012) by Tan et al., was developed to overcome the shortcomings of the GHE technique. CLAHE is designed to suppress noise and unwanted over enhancement in an image. CLAHE is done by separating the original image into non- overlap sub- blocks while enhancing each subblocks solely and recombines the sub- block image using bilinear interpolation. In ELEAHE, the image is separated into sub- blocks. The extreme levels of the sub-block image are eliminated before performing redistribution of pixels and the image blocking effects are reduced using the bilinear interpolation. Enhancing the noise in the image is the drawback of both techniques (ELEAHE and CLAHE). The other group of contrast enhancement technique is the transformation or frequency domain technique which decomposes the image into the frequency domain such as the discrete wavelet transform (DWT), Fourier transform (FT) and discrete Fourier transform (DFT).

3.5 Mathematical Formulation

Image data along the boundary of target structure are extracted and transformed to a rectangular image space where the target boundary is roughly straightened. Resampling the input image along the non-uniform direction was also applied in this process creates an optimal region of interest in which features are mostly oriented in a single direction. A curvilinear prior shape of a model corresponding to the boundary of target structure is used. Then the normal vector which is perpendicular to the prior shape at each point is calculated. The straightened region is then extracted along the normal vectors and transformed into a rectangular boundary image. This simplifies segmentation by optimizing the edge detection in a single direction.

3.6 Transformation of input image to SBI

In this section, we review the SBI creation and propose a new modification for MATLAB implementation of the method. As stated in [31], the SBI is created by a coordinate transformation along a prior shape (PS) from the input image. The PS data is a set of n positive integer pairs showing the coordinates of the PS by the curve C defined as follows:

$$C = \{\cup P_i\, x_i, y_i\, , i = 1, \ldots, n\}$$

For each point of Pi, a corresponding normal vector Ni, which is perpendicular to the PS at each point, is calculated by

$$N_i = N_{xi}, N_{yi}$$

The SBI is created by a transformation from the input image along the PS defined as follows:

$$T_m\, x_i, y_i = (N_x \cdot A_v + xi, Ny \cdot A_v + y_i)$$

where A_v is an acquisition vector that determines the number of samples corresponding to each normal vector. Finally, the transformation Tm is applied in the input image I along the curve C to create the SBI as follows:

$$SBI = I \cdot T_m\, (x_i, y_j\,), x_i, y_j \in C$$

3.7 Redundant and low-resolution data in SBI

As mentioned previously, the SBI is constructed by a transformation in which the normal vector multiplied by an acquisition vector points to the sampling points in the input image. Pixels along a normal vector, which is perpendicular to the PS, are sampled from the original image to create one line of the SBI corresponding to each pixel of the PS. There are some challenging issues in construction of the SBI that are discussed here. The first problem arises when the slope of the PS changes rapidly. As shown, the slope of the PS around the greater trochanter changes rapidly. In this situation, normal vectors converge towards the inside of the object and intersect. This causes that a pixel in this area be sampled by different normal vectors and appears in the SBI in multiple places. If the edges of the object are close to the PS this issue does not cause any problem. However, in the experiments with clinical data, it cannot be guaranteed that the PS is initialised very near the targeted structure. Fig. 2b shows that the PS is a little far from the boundary of the femoral head around the greater trochanter and that its normal vectors intersect causing multiple samples of the edges data. Indeed, the order of edges data can be appeared in the SBI incorrectly. This problem is shown in Fig. 2c where the edge samples d1 and d2 corresponding to the normal vectors at points P1 and P2 are appeared in the SBI in an opposite order to the PS points. The experimental results in these situations show jagged edges and circulation artefact in the final segmentation results shown in Fig. 2d.

When the SBI is constructed, the edge data is extracted by the minimal path algorithm. Then the edge coordinates from the SBI are translated to the coordinates of the original image by a reverse transformation. Here we

propose an algorithm that checks the edge data from the SBI and removes the redundant data which creates artefacts. The proposed algorithm checks validity of the edge data at each line of the SBI and in case of redundancy disqualifies it for reverse transformation. The reverse transformation is applied only on valid and qualified data. The detail of the algorithm is as following.

Assume that the edge data up to point P in was transformed from the SBI to the input image and n_1 is the normal vector at pixel p. This area is depicted in light blue along the PS up to point p and n_2 is the normal vector at q which is the next pixel in the PS. d is the edge data corresponding to n_2 and we will now examine its validity as edge data. The normal vectors n1 and n_2 intersect at point x. If the coordination of d resides in the area, which has already been transformed (blue area), it is considered redundant data and is not transformed to the original image. In the image d is located in the blue area and the algorithm does not transform this data to the input image and proceed to check data correspond to the next normal vector. In this case, the next normal vector is compared with the normal vector corresponding to the last transformed edge data. If the edge is found on the left side of x (in this figure) the data is valid and transformed to the original image. If n_2 is parallel to n_1 or if their intersection point is outside of the blue area the edge data corresponding to n_2 would also qualify.

As opposed to the previous problem of the redundant data, the second problem occurs on the other side of the PS where data is sampled from scattered normal vectors. If an edge is far from the PS and located on a side of the PS where normal vectors diverge, the edge data is sampled with a very low resolution. Fig. 4a shows normal vectors around the corner of the femoral neck and greater trochanter in which the slope of the PS is changed rapidly and the angle between every two consecutive normal vector is significant.

4. SIMULATION RESULTS ANALYSIS

In this research to evaluate the performance of the proposed approach histogram processing of images are evaluated. The images collected from mammogram are evaluated through simulation in MATLAB. Input images are processed using enhanced approach and intensity values are evaluated using cramer-rao approach. By the use of SBI the images are straighten and edge values are identified. The image processing adopted in this research for processing are presented and elaborated in this section.

Parameters	Values
Minimal Pixel Intensity	11
Minimal Cramer Limit	315.039680040467
Minimal Distance	315.039680040467
Maximal Pixel Intensity	38

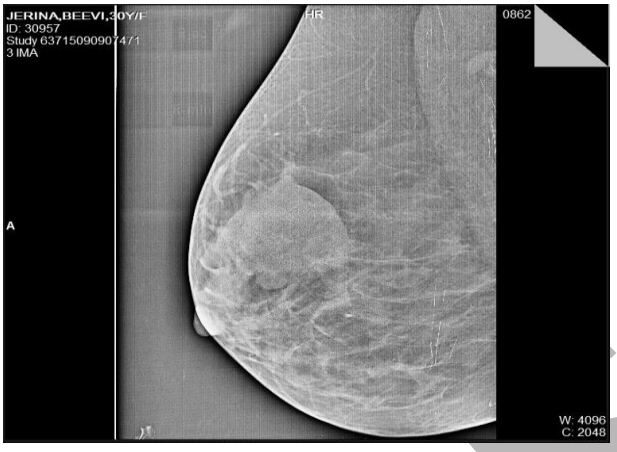

Figure 3: Pre processed Image

The figure 3 illustrates the image preprocessed for processing image with SBI and Cramer-Rao limit conditions. For the processed image the image get smoothened and processed accordingly. Comparison of original image with processed image illustrate that our preprocessing mechanism effectively smoothen monogram images. This pre-processed image is applied as input for Cramer-Rao mechanism with varying pixel intensity value. Based on image pixel intensity different points of image are extracted and segmented for clear dataset identification process. Cramer-rao approach evaluate the input pixel based on

To obtain the reference segmentation for comparison with the automatically obtained results from the Cramer-Rao, the monogram images were peer reviewed in the oncology centre at the head-and-neck radiotherapy weekly team meeting. From that meeting, expert general consensus on the tumour outline on 2D (axial) slices of patients, which is considered as a gold standard in current clinical practice was obtained. In order to analyse inter-variability in manual segmentation,two independent radiation oncologists'(RO1 and RO2), sub-specializing in head-and-neck cancer and with the experience of approximately 10 years, manually outlined the cancer region in all axial slices according to the published guidelines. For intra-variability evaluation both RO1 and RO2 repeated this procedure on the same dataset approximately one month later. The PLCSF results were also compared to RO1 and RO2 outlines.For PLCSF performance assessment, two metrics were utilized; Spatial overlap between two segmentation results was measured using DSC. A high value of DSC (i.e.1) indicates good agreement between two segmentation results. Compared to original Hausdroff distance, MHD reduces impact of outliers and noise and it was used for shape variation evaluation between segmentation.

Figure 4: Image after Cramer- Rao

Segmentation of brease cancer regions is particularly difficult due to the presence of MRI artefacts, enhancements of other non-cancer regions (blood vessels, salivary glands), geometric variability and weak edges of the cancer regions across the patients. An cramer-rao based SBI framework was presented in this paper for this task that does not require any manual intervention or training data. This framework makes no assumption about the shape or size of the cancer regions, thus can successfully segmentthe cancer regions with geometric variability. Also, the cases used in this study are representative of everyday clinical challenges. In this framework, a novel adaptive determination of parameter spline distance (knot spacing) allowed the estimation of complex bias field (IIH) present in monogram slices used in this work. Detection of the throat region using fuzzy rule based technique allowed the knowledge of the approximate cancerous position to be embedded in the system, particularly in MFCM, thus reducing further processing steps to eliminate healthy tissues from cancer detected clusters that are away from the throat region. Comparison of MFCM with the standard SBI showed that MFCM achieved better results compared to the standard SBI. The continuity and spatial smoothness of the cancer boundary was ensured by evolving the level set surface on the detected cancer region. Quantitative comparison with the Gold Standard (consensus manual outline) on 102 T1 + Gd MRI axial slices from 10 patients, the system (PLCSF) shows no significant difference in performance (PCC: 0.89, $p < 0.05$) with the method used in current clinical practice. The PLCSF result also demonstrated improved performance when compared to other algorithms (MS clustering and Ncut). Existing semi-automatic approach [6] for tongue cancer segmentation validated on 16 patients (78 axial slices) demonstrated mean correspondence ratio of 0.83 which is comparable to PLCSF DSC of 0.79. However, the semi-automatic approach in required manual-placing of seed points in the tongue tumour region or drawing of close loop outside the tumour from expert and have no results to prove any validation on laryngeal cancer. The limitation of the current framework (PLCSF) is oversegmentation of cancer region in case of similar characteristics of cancer tissues as compared to surrounding tissues.

Figure 5. Image with Straighten Image condition

One of the main purposes of the automatic cancer region segmentation of T1 + Gd MRI slices is the reproducibility of the segmentation results that contain intra- and inter- variability from manual segmentation results. For this framework, if the parameters values are unchanged, the system obtains similar results for repeated number of times, indicating the reproducibility of the system. Further, using single modality (T1 + Gd) in RTP can reduce scanning and processing time of MRI slices and increase the computational efficiency. Thus, this tool can assist RO in RTP to obtain pharynx and larynx cancer boundaries from T1 + Gd MRI axial slices in time-effective and unbiased manner. To the best of our knowledge this is first automatic tool focused on segmentation of BoT and larynx cancer from T1 + Gd MRI. The system also demonstrated that it can perform robustly against variations caused by different MRI scanners protocols with different manufacturer and scanner models.

5.CONCLUSION AND FUTURE ENHANCEMENT

An image improvement technique is developing for earlier disease detection and treatment stages; the time factor was taken in account to discover the abnormality issues in target images. Image quality and accuracy is the core factors of this research, image quality assessment as well as enhancement stage where were adopted on low pre-processing techniques based on Gabor filter within Gaussian rules. The proposed technique is efficient for segmentation principles to be a region of interest foundation for feature extraction obtaining. The proposed technique gives very promising results comparing with other used techniques. In future based on the collected dataset optimization based approach will be developed for effective detection of cancer affected part.

REFERENCES

[1]. Koh, N. C. Y., Sim, K. S., & Tso, C. P. (2016, November). CT brain lesion detection through combination of recursive sub-image histogram equalization in wavelet domain and adaptive gamma correction with weighting distribution. In *Robotics, Automation and Sciences (ICORAS), International Conference on* (pp. 1-6). IEEE.

[2]. Mundhada, S. O., & Shandilya, V. K. (2012). Spatial and transformation domain techniques for image enhancement. *International Journal of Engineering Science and Innovative Technology (IJESIT)*, *1*(2), 213-16.

[3]. Lidong, H., Wei, Z., Jun, W., & Zebin, S. (2015). Combination of contrast limited adaptive histogram equalisation and discrete wavelet transform for image enhancement. *IET Image Processing*, *9*(10), 908-915.

[4]. Tan, T. L., Sim, K. S., & Chong, A. K. (2012, February). Contrast enhancement of CT brain images for detection of ischemic stroke. In *Biomedical Engineering (ICoBE), 2012 International Conference on* (pp. 385-388). IEEE.

[5]. Huang, S. C., Cheng, F. C., & Chiu, Y. S. (2013). Efficient contrast enhancement using adaptive gamma correction with weighting distribution. *IEEE Transactions on Image Processing*, *22*(3), 1032-1041.

[6] .Pizer, S. M., Amburn, E. P., Austin, J. D., Cromartie, R., Geselowitz, A., Greer, T., ... & Zuiderveld, K. (1987). Adaptive histogram equalization and its variations. *Computer vision, graphics, and image processing*, *39*(3), 355-368.

[7]. Tan, T. L., Sim, K. S., Tso, C. P., & Chong, A. K. (2012). Contrast enhancement of computed tomography images by adaptive histogram equalization-application for improved ischemic stroke detection. *International Journal of Imaging Systems and Technology*, *22*(3), 153-160.

[8]. Radhiyah, A., Harsono, T., & Sigit, R. (2016, November). Comparison study of Gaussian and histogram equalization filter on dental radiograph segmentation for labelling dental radiograph. In *Knowledge Creation and Intelligent Computing (KCIC), International Conference on* (pp. 253-258). IEEE.

[9]. Vidya, V. K., & Mathew, S. (2016, July). An accurate method of breast cancer detection from ultra sound images using probabilistic fuzzy clustering algorithm. In *Communication Systems and Networks (ComNet), International Conference on* (pp. 231-235). IEEE.

[10]. Huynh, P. T., Jarolimek, A. M., & Daye, S. (1998). The false-negative mammogram. *Radiographics*, *18*(5), 1137-1154.

[11]. Rose, C. J., & Taylor, C. J. (2003). A statistical model of texture for medical image synthesis and analysis. *Med. Image Understand. Anal*, 1-4.

[12]. Brockway, J., Subramanian, K., Carruthers, W., & Insko, E. (2004). Detection and visualization of inflammatory breast lesions using dynamic contrast enhanced MRI volumes. *Memory Testing Corp., Charlotte, NC, USA*.

[13].Abbosh, Y. M. (2014). Breast cancer diagnosis using microwave and hybrid imaging methods. *International Journal of Computer Science and Engineering Survey*, *5*(3), 41.

[14].Campisi, M. S., Barbre, C., Chola, A., Cunningham, G., Woods, V., & Viventi, J. (2014, August). Breast cancer detection using high-density flexible electrode arrays and electrical impedance tomography. In *Engineering in Medicine and Biology Society (EMBC), 2014 36th Annual International Conference of the IEEE* (pp. 1131-1134). IEEE..

[15].Tan, T., Platel, B., Huisman, H., Sanchez, C. I., Mus, R., & Karssemeijer, N. (2012). Computer-aided lesion diagnosis in automated 3-D breast ultrasound using coronal spiculation. *IEEE transactions on medical imaging*, *31*(5), 1034-1042.

[16].Hoon, M., & Yap, M. (2008). A novel algorithm for initial lesion detection in ultrasound breast images.

[17].Vidya, V. K., & Mathew, S. (2016, July). An accurate method of breast cancer detection from ultra sound images using probabilistic fuzzy clustering algorithm. In *Communication Systems and Networks (ComNet), International Conference on* (pp. 231-235). IEEE.

[18].Su, Y., Wang, Y., Jiao, J., & Guo, Y. (2011). Automatic detection and classification of breast tumors in ultrasonic images using texture and morphological features. *The open medical informatics journal*, *5*(1).

[19].Kusakunniran, W., Rattanachoosin, J., Sutassananon, K., & Anekkitphanich, P. (2016, November). Automatic quality assessment and segmentation of diabetic retinopathy images. In Region 10 Conference (TENCON), 2016 IEEE (pp. 997-1000). IEEE.

[20].Wen, H., Qi, W., & Shuang, L. (2016, August). Medical X-Ray Image Enhancement Based on Wavelet Domain Homomorphic Filtering and CLAHE. In Robots & Intelligent System (ICRIS), 2016 International Conference on (pp. 249-254). IEEE.

[21].Kaur, H., & Rani, J. (2016, March). MRI brain image enhancement using Histogram Equalization techniques. In Wireless Communications, Signal Processing and Networking (WiSPNET), International Conference on (pp. 770-773). IEEE.

[22].Shajy, L., Smitha, P., & Marichami, P. (2014, December). Enhancement of sputum cytology images through recursive mean separate histogram equalization and SVM classification. In Computational Intelligence and Computing Research (ICCIC), 2014 IEEE International Conference on (pp. 1-5). IEEE.

[23].Huang, L., Wu, C., Chen, L., & Zhu, L. (2013, December). Comparisons of Encryption Algorithms in Histogram-Equalized Image. In Networking and Distributed Computing (ICNDC), 2013 Fourth International Conference on (pp. 80-81). IEEE.